Human Molecular Genetics, 2010, Vol. 19, No. 12 **2433–2444**
doi:10.1093/hmg/ddq126
Advance Access published on March 25, 2010

Zebrafish models of collagen VI-related myopathies

W.R. Telfer[1], A.S. Busta[1,2], C.G. Bonnemann[3], E.L. Feldman[1] and J.J. Dowling[1,2,*]

[1]Department of Neurology and [2]Department of Pediatrics, University of Michigan Medical Center, Ann Arbor, MI 48109-2200, USA and [3]Department of Pediatric Neurology, Children's Hospital of Philadelphia, Philadelphia, PA 19104, USA

Received February 9, 2010; Revised and Accepted March 23, 2010

Collagen VI is an integral part of the skeletal muscle extracellular matrix, providing mechanical stability and facilitating matrix-dependent cell signaling. Mutations in collagen VI result in either Ullrich congenital muscular dystrophy (UCMD) or Bethlem myopathy (BM), with UCMD being clinically more severe. Recent studies demonstrating increased apoptosis and abnormal mitochondrial function in *Col6a1* knockout mice and in human myoblasts have provided the first mechanistic insights into the pathophysiology of these diseases. However, how loss of collagen VI causes mitochondrial dysfunction remains to be understood. Progress is hindered in part by the lack of an adequate animal model for UCMD, as knockout mice have a mild motor phenotype. To further the understanding of these disorders, we have generated zebrafish models of the collagen VI myopathies. Morpholinos designed to exon 9 of *col6a1* produced a severe muscle disease reminiscent of UCMD, while ones to exon 13 produced a milder phenotype similar to BM. UCMD-like zebrafish have increased cell death and abnormal mitochondria, which can be attenuated by treatment with the proton pump modifier cyclosporin A (CsA). CsA improved the motor deficits in UCMD-like zebrafish, but failed to reverse the sarcolemmal membrane damage. In all, we have successfully generated the first vertebrate model matching the clinical severity of UCMD and demonstrated that CsA provides phenotypic improvement, thus corroborating data from knockout mice supporting the use of mitochondrial permeability transition pore modifiers as therapeutics in patients, and providing proof of principle for the utility of the zebrafish as a powerful preclinical model.

INTRODUCTION

Abnormalities in the extracellular matrix are common in human muscular dystrophies (1). Stable attachments between the matrix and the receptors on the surface of the sarcolemmal membrane are required for providing mechanical stability to the contracting muscle fiber. These contacts are also important for mediating signal transduction events that regulate diverse cellular processes, including muscle cell regeneration, proliferation and survival (2).

Collagen VI is an essential component of the myofiber extracellular matrix. Mutations in collagen VI result in two allelic conditions, Ullrich congenital muscular dystrophy (UCMD) and Bethlem myopathy (BM) (3). UCMD is a severe congenital disorder characterized by neonatal hypotonia, weakness and the combination of joint hyperlaxity and severe progressive contractures (4,5). UCMD is associated with significant morbidity and mortality (6). Most patients either never ambulate or lose their ability to do so, and the majority of affected individuals eventually require the need for ventilatory support. Life expectancy is reduced, largely as a result of respiratory failure. BM, on the other hand, is a milder myopathy characterized by later onset, slower progression and largely preserved ambulation (7–9). Patients with BM also exhibit the characteristic combination of initial joint laxity followed by progressive contractures (3,10). The true incidences of UCMD and BM are unknown. Recent studies have shown that UCMD is the second most common congenital muscular dystrophy, accounting for between 20 and 30% of all cases (10).

Collagen VI is a complex macromolecule made up of equal parts of COL6A1, COL6A2 and COL6A3 (11). Collagen VI is

*To whom correspondence should be addressed at: 5019 BSRB, 109 Zina Pitcher Place, University of Michigan, Ann Arbor, MI 48109-2200, USA. Tel: +1 7346479224; Fax: +1 7347637275; Email: jamedowl@med.umich.edu

initially assembled in fibroblasts found throughout the muscle extracellular matrix (3,12,13). Individual collagen VI subunits are combined to form triple helical monomers. These monomers are then assembled into antiparallel dimers, and then into tetramers. The tetrameric collagen VI is secreted into the extracellular milieu. Once outside the fibroblasts, the tetramers are further aligned into microfibrils, which represent the functional collagen VI macromolecule (11,14,15). Microfibrils have been demonstrated to form attachments with several molecules, including other components of the extracellular matrix (biglycan and collagen IV) and adhesion receptors on the surface of the myofiber (integrins) (3,13). One of the main proposed functions for collagen VI is promoting the stability of the sarcolemmal membrane during muscle contractions (1,16). It has also been implicated in a variety of other processes, including basement membrane assembly, and cell signaling events such as cell survival and regulation of myofiber size (3). However, much still remains to be understood about the *in vivo* functions of the collagen VI microfibril.

Mutations in any of the three collagen VI subunits, (COL6A1, COL6A2 and COL6A3), can result in muscle disease (4,5,17). UCMD can result from either recessive or dominant mutations (18,19). Recessive mutations are typically loss of function mutations, with the result being significant reduction in the synthesis of one collagen VI subunit and secondary overall reduction or absence of secreted collagen VI macromolecules (3), although recessive missense mutations have also been described. Heterozygous UCMD mutations, on the other hand, probably act through a dominant-negative mechanism (20,21). They are most often found in exons that code for the N-terminal part of the triple helical domain. They result in collagen VI subunits that can be assembled into monomers, dimers and tetramers, but with impaired ability to be assembled into proper microfibrils. BM was originally characterized as a dominant disorder, although there is clear evidence for recessive inheritance as well (22,23). Mutations in Bethlem most often result in collagen VI subunits that assemble into triple helical monomers, but are not able to be processed further (3). Thus, they reduce the overall amount of collagen VI that is secreted.

Currently, there are no treatments available for either UCMD or BM. Recently, a potential therapeutic avenue has been identified, largely through the use of a mouse model of collagen VI myopathies. This mouse strain has a germline mutation in *Col6a1*, and −/− recessive animals exhibit a very mild clinical myopathy with histopathologically abnormal muscle (24). Irwin *et al*. (25) found abnormalities in the mitochondrial structure and aspects of its function in these mice. Specifically, they observed that the mice had swollen/dilated mitochondria which had lost their normal proton charge gradient, and that these abnormalities in mitochondria led to an increased myofiber apoptosis. They further found that modification in the mitochondrial permeability transition pore (or PTP), either pharmacologically with cyclosporin A (CsA) or genetically by knockout of cyclophilin D, improved the mitochondrial changes and reduced myofiber cell death (25–27). They then found similar abnormalities in the mitochondrial structure and function in patients with collagen VI myopathies, as well as increased cell death (28). This has ultimately lead to the proposed use of PTP modifiers such as CsA or a synthetic analog called debio-025 as treatments for collagen VI myopathies (29,30).

It is currently unclear how interruption of collagen VI function results in abnormalities in mitochondrial function. One proposed mechanism is that tears or leaks in the sarcolemmal membrane, a known phenomenon in collagen VI myopathies, cause a rise in intracellular calcium (29). The increased intracellular calcium causes mitochondrial swelling, which, in turn, disturbs the PTP and leads to the release of the pro-apoptotic factor cytochrome C. This theory has yet to be rigorously tested. Furthermore, it is not known to what extent correction of the mitochondrial abnormalities will affect the disease process in humans. PTP modifiers are not expected to improve the loss of stable extracellular matrix attachments to the muscle membrane and the subsequent disturbance in membrane integrity in UCMD and BM. One big limitation in the preclinical evaluation of the PTP modifiers is the fact that *Col6a1*−/− mice have such an extremely mild phenotype that they are probably best used as a model of mild BM (24). Therefore, although CsA does improve the muscle histology in −/− mice (25), it is difficult to predict what effect it will have in the setting of severe muscle weakness, as seen in the UCMD.

Given the lack of a more robust model for severe collagen VI muscular dystrophies, we generated a model of UCMD using zebrafish. Such a model could then be used as a springboard for future therapeutic studies for treating the severe form of these diseases. Our model uses antisense morpholino technology in the developing zebrafish embryo. Injection of morpholino to zebrafish exon 9 of *col6a1* resulted in an in-frame deletion in the N-terminal part of the triple helical domain, paralleling the dominant mutations in UCMD (31,32). As would be predicted, this morpholino caused a severe myopathy with early-onset development motor deficits and severe ultrastructural changes. Injection of morpholino to exon 13 resulted in an in-frame deletion in the C-terminal part of the triple helical domain, paralleling a typical dominant BM mutation (32,33). This morpholino resulted in a mild myopathy with late-onset motor deficits and obvious histopathologic abnormalities. We further analyzed the exon 9 morpholino to characterize its potential utility as a UCMD model. We observed mitochondrial swelling and increased apoptosis, consistent with the changes observed in patients with UCMD. We tested the effect of CsA in this model, and found that it decreased apoptosis, improved mitochondrial appearance and improved overall motor function. Importantly, we found that the effect of CsA was ‘upstream’ of apoptosis, as correcting apoptosis itself did not improve motor function. On the other hand, the effect was ‘downstream’ of plasma membrane damage, as treatment with CsA did not improve membrane integrity. These results demonstrate that we have successfully developed the first vertebrate model with clinical severity that matches that of UCMD. We provide evidence that PTP modifiers such as CsA can induce functional and structural improvements in this model, and propose that these drugs should be investigated in patients with UCMD.

RESULTS

Morpholino knockdown of zebrafish col6a1

As previously reported, there are single copies in the zebrafish genome of COL6A1, COL6A2 and COL6A3 (34).

We designed morpholinos to exons 9 and 13 of *col6a1*. In human COL6A1, exon 9 is the equivalent of exon 10. Exon 10 encodes a portion of the N-terminal triple helical domain, and it is a common site for dominant mutations in UCMD. Deletion of exon 9 from zebrafish *col6a1* is predicted to result in an in-frame truncated transcript that should function as a dominant negative and generate a UCMD-like phenotype. Injection of exon 9 morpholino into 1–2-cell stage embryos resulted in the reduction of the normal *col6a1* transcript and in the appearance of a novel truncated transcript (Supplementary Material, Fig. S1A, arrow). Direct sequencing of the truncated transcript confirmed an in-frame deletion of exon 9 (data not shown). Exon 13 is the equivalent of exon 14 in human COL6A1. Exon 14 is a commonly deleted exon in BM. Deletion of zebrafish exon 13 is predicted to cause an in-frame deletion that should result in a BM-like phenotype. Injection of exon 13 morpholino resulted in the reduction of normal transcript and the production of an in-frame, truncated transcript (Supplementary Material, Fig. S1B).

Knockdown of zebrafish col6a1 results in developmental motor abnormalities

We analyzed motor function at 24 and 48 h post fertilization (hpf) using two validated motor assays (35): spontaneous coiling (at 24 hpf) and touch-evoked escape response (at 48 hpf). Embryos injected with exon 9 morpholino exhibited severe abnormalities with both assays (Fig. 1A and B). The average number of spontaneous coiling events per 15 s was 1.5 ($\pm$0.4, six trials, $n = 69$) as compared to 7.0 ($\pm$0.4, $n = 138$) for embryos injected with a scrambled control morpholino ($P < 0.0001$; Fig. 1A). The average touch-evoked escape response (as graded on a 0–3 scale; see Materials and Methods section) was 0.3 ($\pm$0.1, 3 trials, $n = 23$) as compared to 2.6 ($\pm$0.1, $n = 66$; $P < 0.0001$; Fig. 1B). Embryos injected with exon 13 morpholino, on the other hand, had normal spontaneous coiling but a mild and statistically significant decrease in touch-evoked escape response. The average number of coiling events was 6.6 ($\pm$0.5, three trials, $n = 82$, $P > 0.05$ when compared with control; Fig. 1A), while the average touch-evoked escape response was 1.8 ($\pm$0.1, 3 trials, $n = 52$, $P < 0.0001$ when compared with controls; Fig. 1B).

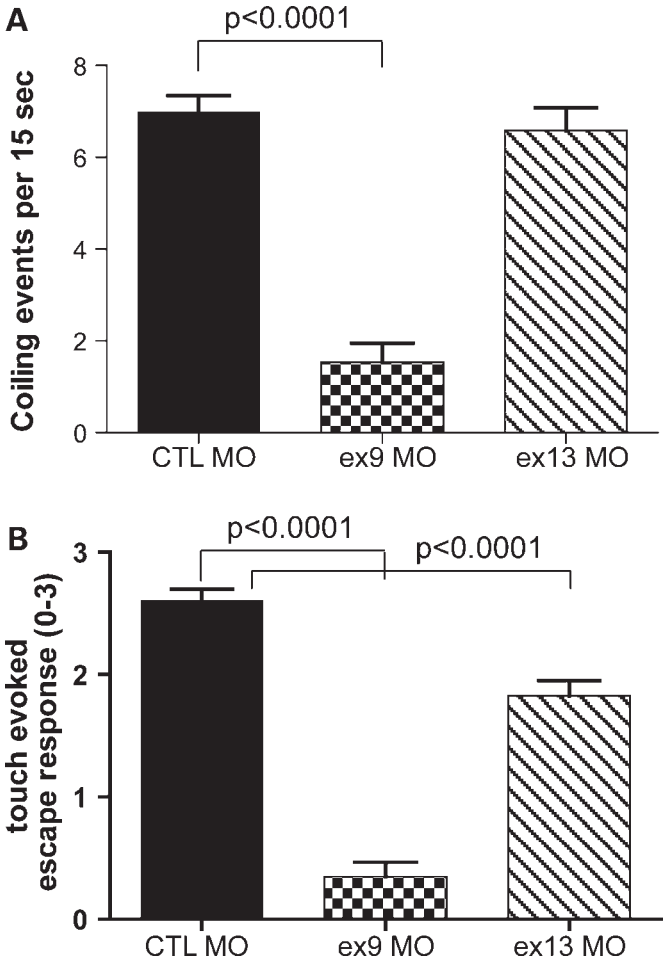

Figure 1. Motor abnormalities in *col6a1* morphant zebrafish. (**A**) Spontaneous coiling as measured at 24 hpf. Exon 9 morphant embryos (ex9 MO) had significant reduction in the number of coiling events observed in 15 s when compared with controls (CTL MO). Exon 13 morphants (ex13 MO) had normal spontaneous coiling. Average values were 7.0 (CTL), 1.5 (ex9) and 6.6 (ex13). (**B**) Touch-evoked escape response as measured at 48 hpf. Exon 9 morphants were severely impaired in this behavior, whereas exon 13 morphants had a mild but statistically significant decrease in activity. Average values were 2.6 (CTL), 0.3 (ex9) and 1.8 (ex13).

Morphologic changes in col6a1 morphants

We then examined morpholino-injected (i.e. morphant) embryos for morphologic changes using live light microscopy. In total, 94.5% of exon 9 morphants exhibited severe abnormalities in their overall appearance ($n = 74$ over five independent injections). At 24 hpf, exon 9 embryos were shorter overall, had hypoplastic midbodies and had bent, foreshortened tails (Fig. 2B). At 48 hpf, these embryos continued to have an obviously dysmorphic appearance. They were substantially shorter than control embryos, had small midbodies and tails and also were often bent into a C-shape (Fig. 2E). Given that the midbody and tail are primarily composed of skeletal muscle compartments, these changes are consistent with a primary muscle pathology and have previously been reported in other zebrafish models of muscular dystrophy and myopathy (35–39). Of note, 84.6% of embryos injected with half concentration of exon 9 morpholino exhibited the same phenotypic (both motor and morphologic) changes ($n = 78$, data not shown).

Injection with exon 13 morpholino, on the other hand, did not result in obvious morphologic changes at either 24 (Fig. 2C) or 48 hpf (Fig. 2F; $n = 82$). This is consistent with the mild motor phenotype detailed above and with our prediction that exon 13 morphants would resemble a BM-like phenotype.

Validation of phenotypic specificity using a col6a3 morpholino

To test the specificity of the changes observed in the *col6a1* morphant embryos for collagen VI disruption, we performed additional experimentation with a morpholino designed to

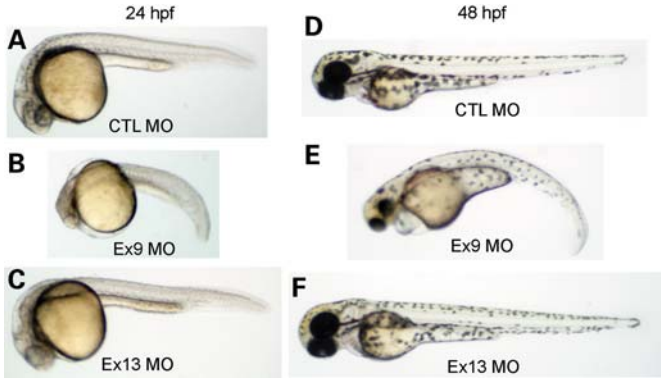

Figure 2. Morphologic abnormalities in *col6a1* morphant zebrafish. Microscopic analysis of live embryos at 24 hpf (**A**–**C**) and 48 hpf (**D**–**F**). Exon 9 morphants were small, with hypoplasic and bent midbodies and tails (B and E). They also had mild pericardial edema, a finding often seen with reduced movement. Exon 13 morphants were grossly normal in appearance at both 24 hpf (C) and 48 hpf (F).

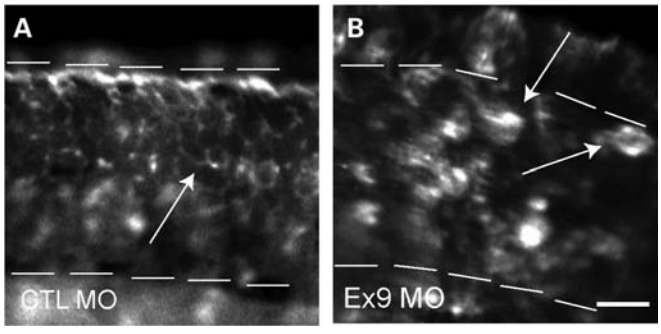

Figure 3. Collagen VI antibody labeling in *col6a1* morphant zebrafish. Whole-mount immunofluorescent analysis was performed on control (CTL MO) and exon 9 (Ex9 MO) morpholino-injected embryos at 48 hpf. CTL MO embryos (**A**) demonstrated a fine, reticulated pattern of staining with their myotomes (arrow). Ex9 MO embryos (**B**), conversely, had diminished staining that was present in unusual patches (arrows). Dashed lines indicate the boundaries of the muscle compartment. $n = 6$ per condition. Scale bar = 1 mm.

exon 9 of the *col6a3* gene. Deletion of exon 9 in zebrafish *col6a3* resulted in an in-frame, truncated transcript that is predicted to function as a dominant-negative mutation (data not shown). This exon is equivalent to human exon 16 of *COL6A3*, and heterozygous deletion of this exon has been reported in several UCMD patients. Morpholino knockdown of exon 9 in *col6a3* caused a severe phenotype with both significant motor deficiencies and widespread morphologic changes (data not shown). The average number of spontaneous coils per 15 s for *col6a3* morphants was 2.6 (± 0.6, $n = 40$) as compared to 7.9 (± 1.2, $n = 21$) for controls ($P < 0.0001$). The phenotype with this morpholino was essentially identical to that observed with the exon 9 *col6a1* morpholino, and demonstrated that the severe morpholino-dependent phenotypes are specific for alterations in collagen VI and not due to non-specific, off-target effects.

Col6a1 morpholino injection alters collagen VI antibody staining

We examined collagen VI antibody staining as an additional test of the specificity of our *col6a1* morpholino. Whole-mount antibody labeling of 48 hpf control embryos with an antibody to collagen VI revealed a fine reticulated pattern in the somatic compartment (arrow, Fig. 3A). Antibody labeling of exon 9 morphant embryos, on the other hand, gave an abnormal pattern of staining. Label was diminished overall and instead found in small clumps scattered throughout the myofiber compartment (Fig. 3B). Such a pattern is consistent with staining previously reported for some UCMD patients with dominant mutations (3).

Col6a1 morphant skeletal muscle exhibits histopathologic alterations

Skeletal muscle from *col6a1* exon 9 and exon 13 morphant embryos was examined by light microscopy at 48 hpf ($n = 4$ embryos per condition). Multiple abnormalities were noted in exon 9 embryos, both at the sarcolemmal membrane and within the myofibers (Fig. 4B). The primary adhesion interface between the extracellular matrix and the plasma membrane in zebrafish muscle is at the myotendinous junction. This junction was nearly unrecognizable in the exon 9 morphants, lacking the dense band of staining seen in controls

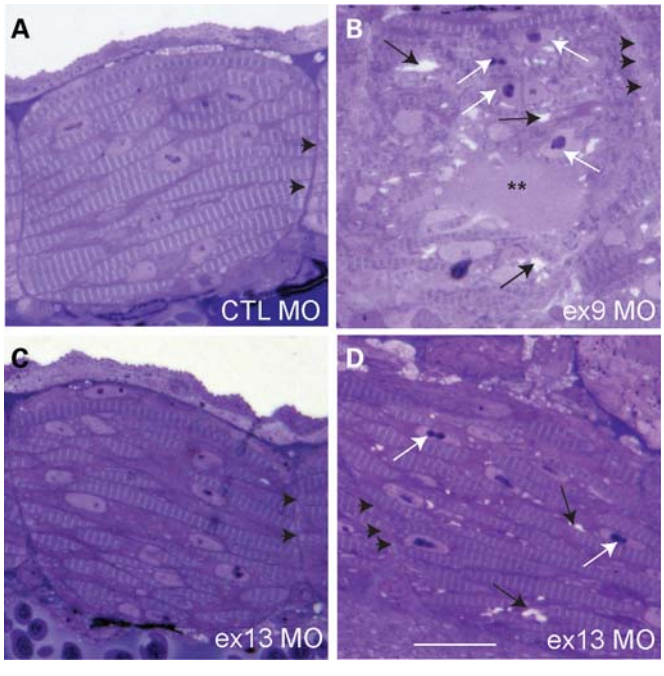

Figure 4. Microscopic abnormalities in *col6a1* morphant zebrafish. Semi-thin sections stained with toluidine blue of 48 hpf zebrafish embryos. Muscle from control morphants is presented in (**A**). In contrast to controls, muscle from exon 9 morphants exhibited multiple changes (**B**). Within the sarcoplasm, these included vacuolated areas (dark arrows), nuclei with condensed chromatin (white areas), and areas of amorphous material (**). In addition, myotendinous junctions were difficult to distinguish and had decreased intensity of staining (arrowheads). Muscle from exon 13 morphants also revealed histologic abnormalities (**C**,**D**). Mild changes were observed in some embryos, and included thinning of the myotendinous junction (arrowheads, C). More severe changes were seen in others (D), and included areas of swelling (black arrows) and nuclei with condensed chromatin (white arrows). Scale bar = 20 mm.

(arrowheads). Within the myofiber itself, multiple small areas that lacked staining were noted (dark arrows, Fig. 4B and D); these probably represent dilated mitochondria and sarcoplasmic reticulum (see below). There were also places of obvious myofiber damage, where normal structure was replaced with opaque, amorphous materials (Fig. 4B, asterisks). In addition, several myonuclei had condensed chromatin, consistent with cells undergoing apoptosis (white arrows). Overall, the findings were consistent with a dystrophic muscle process. Of note, despite these widespread changes, myofibrils (Z bands and actin/myosin cross bridges) were present and appeared normal.

Skeletal muscle from exon 13 morphants exhibited a range of changes. Some myofibers had only subtle histologic abnormalities (Fig. 4C). Other fibers exhibited many of the changes seen in the exon 9 morphants. In particular, areas of hypodensity were observed (arrows), as were nuclei with condensed chromatin (white arrows; Fig. 4D). As with the exon 9 morphants, myofibrils were normal in appearance. However, even in muscle fibers with more obvious structural changes, the myotendinous junctions were less affected, with preservation of some areas of dense staining matrix material (arrowheads).

Col6a1 morphant skeletal muscle has severe ultrastructural abnormalities

Col6a1 morphant embryos have ultrastructural abnormalities that mirror the changes observed by light microscopy ($n = 4$ embryos per condition). Analysis of exon 9 morphants at 48 hpf revealed abnormalities in multiple areas of the myofiber. The most striking intracellular changes were in the mitochondria and the endoplasmic reticulum (ER). When compared with controls, perinuclear mitochondria were large, swollen, and had many fewer distinguishable cristae (Fig. 5A and B). Single membrane structures corresponding to ER were also swollen and enlarged (Fig. 5A and C). These changes are consistent with those observed in *Col6a1* knockout mice and in patients with UCMD (see Supplementary Material, Fig. S2 for comparison) (25,28).

In addition, the myotendinous junctions in exon 9 morphants appeared to be obviously abnormal. The extracellular matrix had a paucity of electron dense material, and the sarcolemmal membrane was thin with numerous small discontinuities (arrow, Fig. 6B). There was also a significant increase in the number of peri-membranous mitochondria (M in Fig. 6C). We quantitated this observation, and found that, on average, there were 16.0 (± 0.6, $n = 8$) mitochondria per high-powered field in exon 9 morphants. Conversely, only 5.8 (± 0.6, $n = 6$) per field were observed in control embryos ($P < 0.0001$).

Exon 13 morphants also exhibited ultrastructural abnormalities (Fig. 6D). Similar, though less dramatic, changes in mitochondria and ER were observed. The myotendinous junction also had decreased electron density (arrow). Severe membrane tears were observed in some places (Fig. 6D, asterisks). These areas of membrane rupture were more extensive than those observed in exon 9 morphants, which may be due to the fact that exon 13 embryos were more active than exon 9 morphants (see Fig. 2), and thus their muscle was exposed to greater mechanical stress.

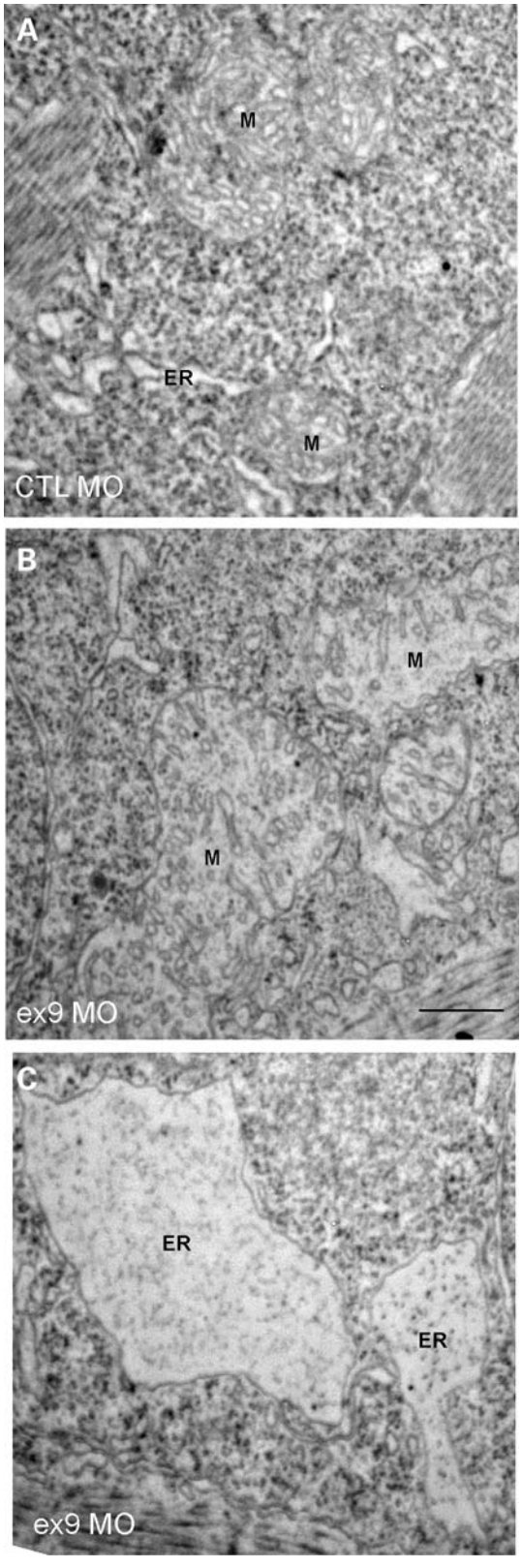

Figure 5. Ultrastructural changes in organelles in *col6a1* exon 9 morphant zebrafish. Electron microscopic analysis on 48 hpf morphant embryos. As compared to controls (**A**), exon 9 morphant embryos have abnormalities in intracellular organelles (**B**,**C**). Specifically, mitochondria are swollen with abnormal cristae (M, B), and endoplasmic reticulum are dilated (ER, C). These changes are consistent with those reported in patients with Ullrich CMD. Scale bar = 500 nm.

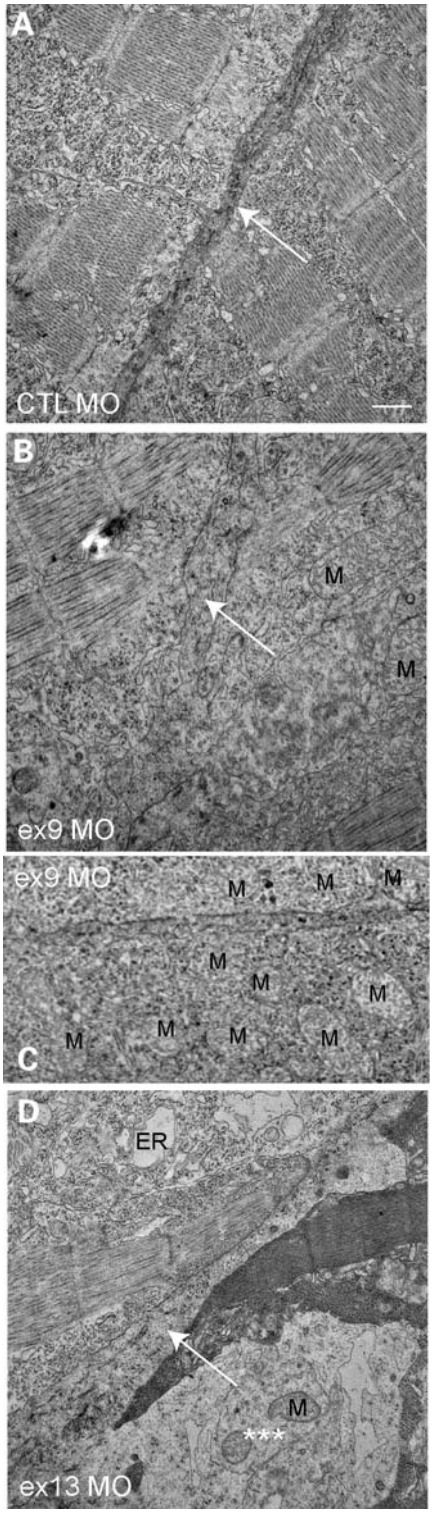

Figure 6. Sarcoplasmic ultrastructural changes in *col6a1* morphant zebrafish. (**A**) Normal myotendinous junction in control morphant embryos (arrow, CTL MO). (**B**) Myotendinous junctions in exon 9 morphants show multiple abnormalities (arrow). The sarcoplasmic membranes are thinned with small rips/breaks, and the surrounding extracellular matrix is broad and less dense. (**C**) An excessive number of mitochondria were present in the submembranous area of exon 9 morphants. (**D**) Ultrastructural changes in exon 13 morphants. These include swollen/dilated endoplasmic reticulum (ER), abnormal myotendonous junctions (arrow) and large areas of subsarcolemmal disorganization (***). Scale bar = 500 nm.

In all, the functional, morphologic and structural changes caused by *col6a1* morpholinos are consistent with a mild, Bethlem-like phenotype (exon 13 morpholino) and with a severe, UCMD-like phenotype (exon 9 morpholino). Because we were most interested in generating and studying a model of UCMD, for the remaining analysis we focused on the exon 9 morphant embryos.

Assessment of apoptosis in col6a1 exon 9 morphant embryos

Histologic examination of *col6a1* exon 9 morphant skeletal muscle suggested that apoptosis was increased in these embryos. We further examined and quantitated this observation using TUNEL staining. Exon 9 morphants had significantly increased numbers of apoptotic myonuclei when compared with controls. Representative TUNEL stained exon 9 and control morphant embryos are depicted in Figure 7A (see also Supplementary Material, Fig. S3). The results of the quantitative analysis are presented in Figure 7B. On average, there were 11.5 ($\pm$2.4, $n = 13$) apoptotic myonuclei in exon 9 morphants versus only 3.2 ($\pm$0.3, $n = 29$) for control morphants ($P < 0.0001$).

It has previously been demonstrated in *col6a1* knockout mice and in UCMD patient myocytes that treatment with CsA reduces the amount of apoptosis (25,28). We therefore tested the effect of CsA on cell death in our zebrafish exon 9 morphants (Fig. 7). As expected, CsA reduced the average number of apoptotic cells from 11.5 to 7.5 ($\pm$1.0, $n = 16$, $P = 0.05$). This result corroborates the effect of CsA on apoptosis seen in mammalian models and thus supports the validity of the exon 9 morphant zebrafish as an accurate model of severe collagen VI myopathy.

Another well-characterized method for reducing apoptosis in zebrafish is knockdown of the p53 tumor suppressor gene using a p53-specific morpholino (40). Co-injection of the p53 morpholino with the exon 9 morpholino also reduced apoptosis from 11.5 to 6.2 ($\pm$1.2, $n = 25$, $P = 0.01$; Fig. 7B). There was no statistical difference in the reduction in apoptosis between p53 knockdown and CsA treatment, as well as no difference in apoptosis between either condition alone and p53 morpholino + CsA treatment (Fig. 7B).

CsA treatment improves motor function in col6a1 exon 9 morphants

To determine the effect of CsA treatment on the severely impaired motor function in exon 9 morphant embryos, embryos were injected with morpholino at the 1–2-cell stage, dechorionated at 20 hpf, treated with CsA for 3 h (21–24 hpf), and then analyzed for spontaneous coiling at 24 hpf (Fig. 8). We observed an obvious improvement in spontaneous coiling after only 3 h of treatment. CsA-treated embryos had, on average, 4.1 coiling events in 15 s ($\pm$0.7, $n = 30$), as compared to 1.2 events in vehicle (DMSO)-treated exon 9 morphants ($\pm$1.2, $n = 27$, $P = 0.003$). Recovery was not complete, however, as exon 9 morphants treated with CsA still had reduced movements when compared with DMSO-treated embryos (4.1 versus 6.8, $n = 35$ for controls, $P = 0.009$). Remarkably, CsA not only improved the overall

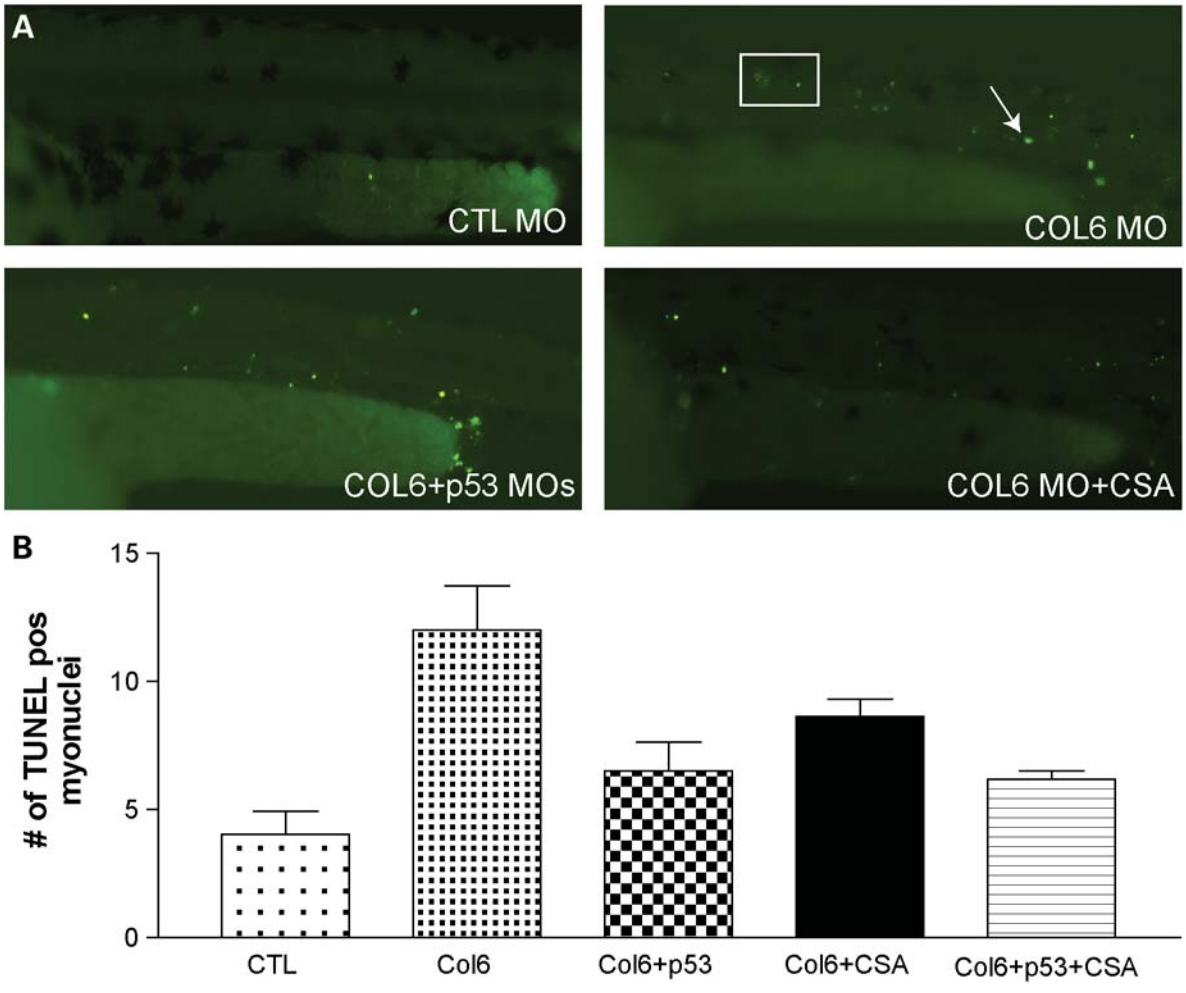

Figure 7. Apoptosis in *col6a1* morphant zebrafish. (**A**) Representative images of whole-mount TUNEL staining on morphant embryos. Control embryos (CTL MO) have very few TUNEL-positive cells. Exon 9 morphants (COL6) have an increased number of TUNEL-positive cells. Boxed cells and those indicated by the arrow are positive myonuclei. The number of positive cells is reduced in exon 9 morphants by co-injection with p53 morpholino (COL6 + p53 MOs) or by treatment with cyclosporin A (COL6 MO+ CsA). (**B**) Quantitation of TUNEL-positive myonuclei. An average number of positive cells are as follows: CTL = 3.2, COL6 = 11.5, COL6 + p53 = 6.2, COL6 + CsA = 7.5, and COL6 + CsA + p53 = 6.2.

number of coiling events, but also significantly reduced the percentage of completely paralyzed embryos (DMSO versus CsA, 59 ± 7% versus 33 ± 6%, $P = 0.006$).

To test whether the effect of CsA was solely a result of its anti-apoptotic properties, we compared motor function of CsA-treated embryos with those co-injected with p53 and exon 9 morpholinos (Fig. 8). Despite the significant reduction in apoptosis caused by p53 knockdown (see Fig. 4B), double morphant embryos did not show improvement in spontaneous coiling (DMSO versus p53, 1.2 versus 1.2, $n = 29$ for exon 9 + p53). Also, there was no significant difference in motor function of exon 9 morphants between CsA treatment and CsA treatment + p53 morpholino injection (data not shown).

CsA treatment improves the ultrastructural appearance of exon 9 morphants

CsA treatment would be predicted to improve the appearance of mitochondria in exon 9 morphant skeletal muscle (25). We performed electron microscopic analysis of CsA and vehicle-treated exon 9 morphant embryos to test this (Fig. 9). CsA-treated morphant embryos had clear improvements in their mitochondria (Fig. 9B). The mitochondria were less swollen and had an increase in the density and complexity of their cristae. DMSO-treated morphants, on the other hand, had swollen, dysmorphic mitochondria that were indistinguishable in appearance from those seen with exon 9 morpholino alone (Fig. 9A, and see Fig. 3). Similar improvement in mitochondria appearance has been described with CsA treatment of *Col6a1* knockout mice (25).

CsA treatment does not improve sarcolemmal membrane appearance and overall myofiber integrity

We finally assessed the effect of CsA treatment on the structural appearance of the sarcolemmal membrane and on overall myofiber integrity. As shown in Figures 2 and 3, the sarcolemmal membrane and the surrounding extracellular

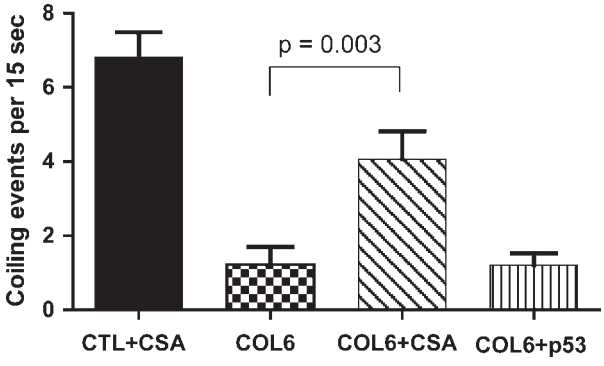

Figure 8. Cyclosporin A improves motor function in *col6a1* morphant zebrafish. Embryos were injected with morpholino at the 1–4-cell stage, treated with either DMSO or cyclosporin A (CsA) from 21 to 24 h post fertilization, and then examined by measuring spontaneous coiling. Values were as follows: CTL + CsA = 6.8, COL6 + DMSO = 1.2, COL6 + CsA = 4.1, COL6 + p53 = 1.2. (CTL = control morpholino and COL6 = *col6a1* exon 9 morpholino).

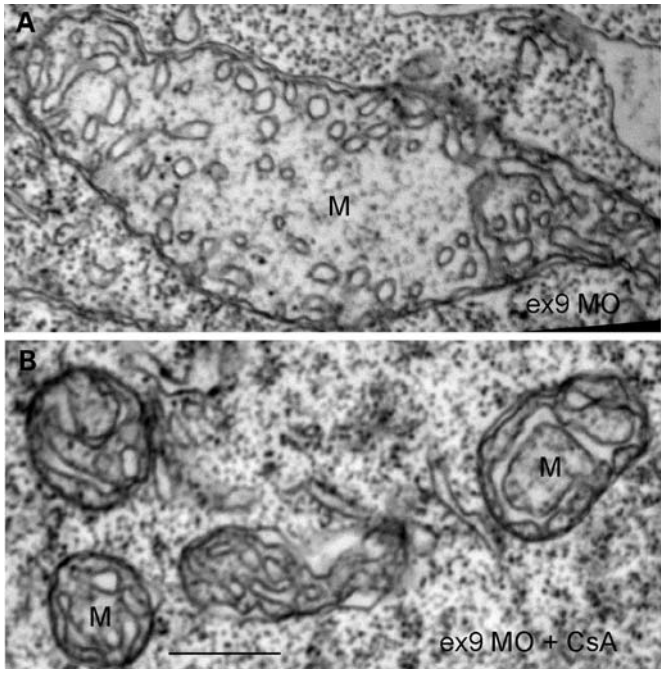

Figure 9. Cyclosporin A improves organelle ultrastructural appearance in COL6A1 morphants. COL6A1 exon 9 morphant embryos were treated either with DMSO or cyclosporin A (CsA). DMSO-treated embryos display mitochondrial and endoplasmic reticular swelling. CsA treatment essentially rescues these organellar abnormalities. M = mitochondria. Scale bar = 500 nm.

matrix are severely disturbed in exon 9 morphants. We examined the myotendinous junctions in CsA and DMSO-treated exon 9 morphant embryos, using electron microscopy. We found no obvious differences between them, detecting similar abnormalities to those seen with exon 9 morpholino injection alone (data not shown).

We also evaluated the effect of CsA on myofiber integrity and organization using a quantitative assessment of skeletal muscle birefringence. Birefringence, the reflected appearance of muscle under polarized light, is a normal property of intact muscle that indicates proper myofiber organization and is a surrogate measure of myofiber integrity (37). Reduced birefringence has been reported in several zebrafish models of muscular dystrophy (36,37). Embryos injected with exon 9 morpholino have significantly reduced birefringence (as measured at 48 hpf), consistent with the dystrophic changes observed by electron microscopy (Fig. 6). Birefringence is easily quantified by measuring the mean intensity of a fixed portion of the embryo (Fig. 10). Exon 9 morphants had an average birefringence intensity of 30.5 ($\pm$3.1, $n = 21$). Conversely, control embryos had an average intensity of 128.7 ($\pm$16.4, $n = 21$, $P < 0.0001$). To determine the effect of CsA treatment on membrane integrity, we measured the mean intensity of birefringence in treated embryos. The average value was 42.1 ($\pm$8.7, $n = 21$), a value that was not statistically different from untreated exon 9 morphants ($P = 0.2$). As with untreated embryos, this value was also significantly lower than that measured for control embryos ($P < 0.0001$).

DISCUSSION

Both BM and UCMD are allelic conditions caused by abnormalities in collagen VI and characterized by the combination of weakness, hypermobility and contractures (3). UCMD is the second most common congenital muscular dystrophy and is associated with progressive symptoms and with significant morbidity and mortality (6,10). No current treatments exist for either condition, and an animal model that mirrors the severity of UCMD is lacking. We present here the first vertebrate model with a severe motor phenotype that equates with UCMD. We used antisense morpholino technology to generate zebrafish embryos with dominant-negative transcripts of *col6a1* that result in severe morphologic, structural and functional changes.

The validity of our zebrafish model is supported by several observations. The first is that many of the ultrastructural changes that have been reported in patients with collagen VI myopathies were observed in the skeletal muscle of morphant embryos, including swelling and dilation of the mitochondria and ER (29). These pathologic findings, also present in the muscle of *Col6a1* knockout mice, are relatively unique to BM and UCMD patients, and are not a common feature of all congenital muscular dystrophies (25). They have been reported, however, in congenital muscular dystrophy due to mutation in the *LAMA2* gene (27). Another consistent finding was the increase in cell death observed in the morphant zebrafish. Increased apoptosis is a well-characterized phenomenon in collagen VI myopathy patient biopsy samples (28). A third observation is the gradation of severity observed with our two morpholinos. We predicted that the exon 9 morpholino would have a severe, 'UCMD-like' phenotype, whereas the exon 13 morpholino would have a mild, 'Bethlem-like' phenotype. These predictions were based on the knowledge of how the COL6A1 protein is processed and assembled into the maturing collagen VI macromolecule and also on information from known patient mutations (3,14,21,31,32,41). Our morpholinos behaved essentially as predicted, with the exon 9 morpholino causing a very severe phenotype and the exon

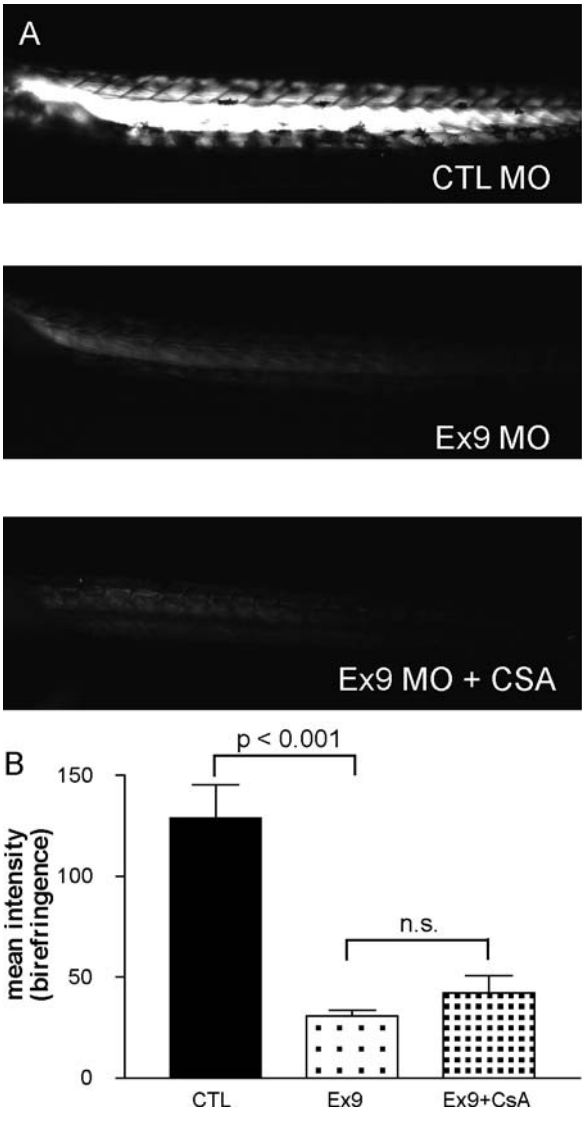

Figure 10. Abnormal birefringence in *col6a1* morphants is not improved with cyclosporin A treatment. (**A**) Birefringence in control morphants (CTL MO), exon 9 morphants (Ex9 MO) and exon 9 morphants treated with cyclosporin A (Ex9 MO + CsA). (**B**) Birefringence is significantly reduced in exon 9 morphants, an abnormality which is not improved with cyclosporin A treatment.

13 morpholino producing a mild, later onset motor deficit. The final observation that supports the validity of our model is the response to CsA. As also seen in patient biopsy samples and in *Col6a1* knockout mice (29), CsA treatment decreases apoptosis and improves the appearance of the mitochondria in our zebrafish morphants.

The morphant zebrafish model shares many similarities to the only previous vertebrate model of collagen VI myopathy, the *Col6a1* knockout mouse (24,25). These mice lack expression of *Col6a1* and make essentially no normal collagen VI. They have many of the structural changes observed in patient biopsies. In fact, it was through the study of *Col6a1* knockout mice that the observations of increased apoptosis and dysfunctional mitochondria in collagen VI myopathies were first made. The prominent limitation of this model, however, is its very mild clinical phenotype. Because of this, the *Col6a1* knockout mouse is probably best considered a model of BM. It is not clear why the mice have such a mild phenotype, as homozygous nonsense or null mutations in *COL6A1* in humans result in a severe clinical picture consistent with a diagnosis of UCMD (18,19).

The mild nature of the clinical changes in the *Col6a1* knockout mice has presented a barrier for therapy development. An example is with CsA and other proton pump modifiers. These drugs clearly improve the structural abnormalities in the knockout mice (25,30), but it is unclear from the mouse studies what effect these drugs would have on more severe disease phenotypes. One of the strengths and unique features of our zebrafish model is that the exon 9 morphant embryos have a severe, early-onset clinical phenotype. This phenotype is very much in line with what would be expected for an animal model of UCMD, and thus therapeutic investigations in our model should provide better insight into the degree of impact that can be expected against more severe disease. We found that CsA improves mitochondrial appearance and decreases apoptosis in the more severely affected zebrafish morphants, similar to what has been reported for the more mildly affected mouse model. CsA provides a partial rescue of the severe clinical phenotype, reducing the number of paralyzed embryos. This demonstrated functional benefit lends support to the hypothesis that proton pump modifiers may have efficacy in treating humans with severe collagen IV myopathies.

There are several advantages to a zebrafish model of UCMD. In addition to the clinical severity of the model, the fact that zebrafish lend themselves to facile genetic manipulation enables novel insights into disease pathways and mechanisms. This is demonstrated by our studies of CsA. We used a morpholino to knockdown the p53 tumor suppressor gene, which reduced apoptosis to the levels obtained with CsA. Unlike CsA, reducing apoptosis through p53 suppression did not improve the motor phenotype, strongly suggesting that CsA treatment efficacy is not solely the result of reducing mitochondrially mediated apoptosis. Whether, then, the ability of CsA to improve motor function in our model is related to other effects of improving mitochondrial function, or is instead due to additional non-predicted roles of CsA, is unclear. From our experimentation, however, it is clear that this non-apoptosis effect of CsA on motor function is not related to improvements in the structural appearance of the plasma membrane and in overall myofiber integrity. Further work will be necessary to pinpoint the exact interrelationship between CsA and other proton pump modifiers and restoration of muscle function in collagen VI myopathies.

Finally, our work opens up an important new avenue for potential treatment development for UCMD, namely the search for molecules that improve or reduce membrane damage and myofiber disorganization. Small tears or leaks in the plasma membrane are probably one of the initial pathologic events in UCMD (16), and we demonstrate in our zebrafish model that proton pump modifiers such as CsA do not improve this important aspect of the disease pathologensis. We predict that molecules able to improve or restore membrane integrity and/or myofiber organization will have a significant impact on disease pathogenesis. Such molecules

theoretically should work in combination with 'downstream' therapeutics such as CsA. Ongoing work is focused on identifying such compounds, using two other powerful aspects of our model: the high number of affected embryos able to be produced and the presence of an easily measurable and quantifiable assay for myofiber integrity (i.e. birefringence).

Conclusion

In summary, we have used morpholino antisense technology to create zebrafish models of BM and UCMD. These models enabled novel insights into collagen IV-related myopathy pathogenesis, and provide a unique platform for further investigations into drug discovery in these diseases.

MATERIALS AND METHODS

Morpholinos

Morpholinos were designed to exons 9 and 13 of *col6a1* and exon 13 of *col6a1* (GeneTools, Inc). A control morpholino, with no sequence homology in the zebrafish genome, was obtained from GeneTools.

Exon 9, COL6A1: GAGAGCGGAAGACGAACCTTCATTC
Exon 13, COL6A1: AGGTAACAGTAATACTCACATCTGG
Exon 9, COL6A3: ATGATTACTACACACTTACAGGACC
p53: GCGCCATTGCTTTGCAAGAATTG

Morpholino injections

Embryos were isolated after paired matings of AB zebrafish and injected at the 1–2-cell stage using a Drummond Nanoject. Morpholino (4.6 nl each) was injected at a concentration of 0.25 mM (approximate total amount of morpholino injected = 9 ng).

Assays of motor function

Spontaneous coiling was measured at 24 hpf by observing the number of coils in a 15-s period. Touch-evoked escape response was measured at 48 hpf using a scale from 0 to 3: 0, no movement; 1, flicker of movement but no swimming; 2, movement away from probe but with impaired swimming; 3, normal swimming.

Live image analysis

Embryos were photographed at 24 and 48 hpf using a Leica MXIII Stereoscope at ×2 with a ×4 zoom. Embryos were anesthetized using Tricaine prior to photographing.

Histopathologic analysis

Zebrafish of 48 hpf were fixed overnight in Karnovsky's fixative and then processed for embedding in epon by the Microscopy and Imaging Laboratory core facility at the University of Michigan. Semi-thin sections were stained with toluidine blue and photographed using an Olympus BX-51 upright microscope. Electron microscopy was performed using a Phillips CM-100 transmission electron microscope.

Whole-mount immunofluorescence

Labeling was performed as described previously, using 48 hpf embryos and a rabbit polyclonal antibody to collagen VI (1:50; Abcam) (42).

TUNEL staining

TUNEL was performed on 48 hpf embryos with the ApopTag kit using manufacturers' instructions (Chemicon International).

CsA treatment

Morphant embryos were dechorionated at 20 hpf and then incubated in CsA from 21 to 24 hpf. CsA was used at 100 μM and dissolved in 0.1% DMSO in egg water. Vehicle control treatment consisted of 0.1% DMSO in egg water.

Birefringence

Birefringence was measured on 48 hpf embryos anesthetized using tricaine. It was measured using two polarizing filters on a Nikon AZ-100 microscope and the NIS Elements software package (Nikon).

Statistical analysis

Statistical analysis was performed on relevant data using Student's two-tailed *t*-test and the Prism GraphPad software package.

SUPPLEMENTARY MATERIAL

Supplementary Material is available at *HMG* online.

ACKNOWLEDGEMENTS

Assistance with electron microscopy was provided by the Microscopy and Imaging Laboratory (MIL) at the University of Michigan.

Conflicts of Interest statement. None declared.

FUNDING

This work was supported by the National Institutes of Health [1K08AR054835 to J.J.D.], by the A. Alfred Taubman Medical Research Institute and the Program for Neurology Research and Discovery. Funding to pay the Open Access publication charges for this article was provided by Department of Pediatrics at the University of Michigan.

REFERENCES

1. Schessl, J., Zou, Y. and Bonnemann, C.G. (2006) Congenital muscular dystrophies and the extracellular matrix. *Semin. Pediatr. Neurol.*, **13**, 80–89.
2. Lapidos, K.A., Kakkar, R. and McNally, E.M. (2004) The dystrophin glycoprotein complex: signaling strength and integrity for the sarcolemma. *Circ. Res.*, **94**, 1023–1031.
3. Lampe, A.K. and Bushby, K.M. (2005) Collagen VI related muscle disorders. *J. Med. Genet.*, **42**, 673–685.
4. Bertini, E. and Pepe, G. (2002) Collagen type VI and related disorders: Bethlem myopathy and Ullrich scleroatonic muscular dystrophy. *Eur. J. Paediatr. Neurol.*, **6**, 193–198.
5. Mercuri, E., Yuva, Y., Brown, S.C., Brockington, M., Kinali, M., Jungbluth, H., Feng, L., Sewry, C.A. and Muntoni, F. (2002) Collagen VI involvement in Ullrich syndrome: a clinical, genetic, and immunohistochemical study. *Neurology*, **58**, 1354–1359.
6. Nadeau, A., Kinali, M., Main, M., Jimenez-Mallebrera, C., Aloysius, A., Clement, E., North, B., Manzur, A.Y., Robb, S.A., Mercuri, E. *et al.* (2009) Natural history of Ullrich congenital muscular dystrophy. *Neurology*, **73**, 25–31.
7. Tachi, N., Tachi, M., Sasaki, K. and Imamura, S. (1989) Early-onset benign autosomal-dominant limb-girdle myopathy with contractures (Bethlem myopathy). *Pediatr. Neurol.*, **5**, 232–236.
8. Mohire, M.D., Tandan, R., Fries, T.J., Little, B.W., Pendlebury, W.W. and Bradley, W.G. (1988) Early-onset benign autosomal dominant limb-girdle myopathy with contractures (Bethlem myopathy). *Neurology*, **38**, 573–580.
9. Jobsis, G.J., Boers, J.M., Barth, P.G. and de Visser, M. (1999) Bethlem myopathy: a slowly progressive congenital muscular dystrophy with contractures. *Brain*, **122**(Pt 4), 649–655.
10. Okada, M., Kawahara, G., Noguchi, S., Sugie, K., Murayama, K., Nonaka, I., Hayashi, Y.K. and Nishino, I. (2007) Primary collagen VI deficiency is the second most common congenital muscular dystrophy in Japan. *Neurology*, **69**, 1035–1042.
11. Engvall, E., Hessle, H. and Klier, G. (1986) Molecular assembly, secretion, and matrix deposition of type VI collagen. *J. Cell Biol.*, **102**, 703–710.
12. Zou, Y., Zhang, R.Z., Sabatelli, P., Chu, M.L. and Bonnemann, C.G. (2008) Muscle interstitial fibroblasts are the main source of collagen VI synthesis in skeletal muscle: implications for congenital muscular dystrophy types Ullrich and Bethlem. *J. Neuropathol. Exp. Neurol.*, **67**, 144–154.
13. Wiberg, C., Klatt, A.R., Wagener, R., Paulsson, M., Bateman, J.F., Heinegard, D. and Morgelin, M. (2003) Complexes of matrilin-1 and biglycan or decorin connect collagen VI microfibrils to both collagen II and aggrecan. *J. Biol. Chem.*, **278**, 37698–37704.
14. Colombatti, A., Mucignat, M.T. and Bonaldo, P. (1995) Secretion and matrix assembly of recombinant type VI collagen. *J. Biol. Chem.*, **270**, 13105–13111.
15. Kuo, H.J., Keene, D.R. and Glanville, R.W. (1995) The macromolecular structure of type-VI collagen. Formation and stability of filaments. *Eur. J. Biochem.*, **232**, 364–372.
16. Kanagawa, M. and Toda, T. (2006) The genetic and molecular basis of muscular dystrophy: roles of cell–matrix linkage in the pathogenesis. *J. Hum. Genet.*, **51**, 915–926.
17. Pepe, G., Bertini, E., Bonaldo, P., Bushby, K., Giusti, B., de Visser, M., Guicheney, P., Lattanzi, G., Merlini, L., Muntoni, F. *et al.* (2002) Bethlem myopathy (BETHLEM) and Ullrich scleroatonic muscular dystrophy: 100th ENMC international workshop, 23–24 November 2001, Naarden, The Netherlands. *Neuromuscul. Disord.*, **12**, 984–993.
18. Camacho Vanegas, O., Bertini, E., Zhang, R.Z., Petrini, S., Minosse, C., Sabatelli, P., Giusti, B., Chu, M.L. and Pepe, G. (2001) Ullrich scleroatonic muscular dystrophy is caused by recessive mutations in collagen type VI. *Proc. Natl Acad. Sci. USA*, **98**, 7516–7521.
19. Giusti, B., Lucarini, L., Pietroni, V., Lucioli, S., Bandinelli, B., Sabatelli, P., Squarzoni, S., Petrini, S., Gartioux, C., Talim, B. *et al.* (2005) Dominant and recessive COL6A1 mutations in Ullrich scleroatonic muscular dystrophy. *Ann. Neurol.*, **58**, 400–410.
20. Pan, T.C., Zhang, R.Z., Sudano, D.G., Marie, S.K., Bonnemann, C.G. and Chu, M.L. (2003) New molecular mechanism for Ullrich congenital muscular dystrophy: a heterozygous in-frame deletion in the COL6A1 gene causes a severe phenotype. *Am. J. Hum. Genet.*, **73**, 355–369.
21. Pace, R.A., Peat, R.A., Baker, N.L., Zamurs, L., Morgelin, M., Irving, M., Adams, N.E., Bateman, J.F., Mowat, D., Smith, N.J. *et al.* (2008) Collagen VI glycine mutations: perturbed assembly and a spectrum of clinical severity. *Ann. Neurol.*, **64**, 294–303.
22. Jobsis, G.J., Keizers, H., Vreijling, J.P., de Visser, M., Speer, M.C., Wolterman, R.A., Baas, F. and Bolhuis, P.A. (1996) Type VI collagen mutations in Bethlem myopathy, an autosomal dominant myopathy with contractures. *Nat. Genet.*, **14**, 113–115.
23. Merlini, L., Martoni, E., Grumati, P., Sabatelli, P., Squarzoni, S., Urciuolo, A., Ferlini, A., Gualandi, F. and Bonaldo, P. (2008) Autosomal recessive myosclerosis myopathy is a collagen VI disorder. *Neurology*, **71**, 1245–1253.
24. Bonaldo, P., Braghetta, P., Zanetti, M., Piccolo, S., Volpin, D. and Bressan, G.M. (1998) Collagen VI deficiency induces early onset myopathy in the mouse: an animal model for Bethlem myopathy. *Hum. Mol. Genet.*, **7**, 2135–2140.
25. Irwin, W.A., Bergamin, N., Sabatelli, P., Reggiani, C., Megighian, A., Merlini, L., Braghetta, P., Columbaro, M., Volpin, D., Bressan, G.M. *et al.* (2003) Mitochondrial dysfunction and apoptosis in myopathic mice with collagen VI deficiency. *Nat. Genet.*, **35**, 367–371.
26. Palma, E., Tiepolo, T., Angelin, A., Sabatelli, P., Maraldi, N.M., Basso, E., Forte, M.A., Bernardi, P. and Bonaldo, P. (2009) Genetic ablation of cyclophilin D rescues mitochondrial defects and prevents muscle apoptosis in collagen VI myopathic mice. *Hum. Mol. Genet.*, **18**, 2024–2031.
27. Millay, D.P., Sargent, M.A., Osinska, H., Baines, C.P., Barton, E.R., Vuagniaux, G., Sweeney, H.L., Robbins, J. and Molkentin, J.D. (2008) Genetic and pharmacologic inhibition of mitochondrial-dependent necrosis attenuates muscular dystrophy. *Nat. Med.*, **14**, 442–447.
28. Merlini, L., Angelin, A., Tiepolo, T., Braghetta, P., Sabatelli, P., Zamparelli, A., Ferlini, A., Maraldi, N.M., Bonaldo, P. and Bernardi, P. (2008) Cyclosporin A corrects mitochondrial dysfunction and muscle apoptosis in patients with collagen VI myopathies. *Proc. Natl Acad. Sci. USA*, **105**, 5225–5229.
29. Bernardi, P. and Bonaldo, P. (2008) Dysfunction of mitochondria and sarcoplasmic reticulum in the pathogenesis of collagen VI muscular dystrophies. *Ann. N. Y. Acad. Sci.*, **1147**, 303–311.
30. Tiepolo, T., Angelin, A., Palma, E., Sabatelli, P., Merlini, L., Nicolosi, L., Finetti, F., Braghetta, P., Vuagniaux, G., Dumont, J.M. *et al.* (2009) The cyclophilin inhibitor Debio 025 normalizes mitochondrial function, muscle apoptosis and ultrastructural defects in Col6a1(−/−) myopathic mice. *Br. J. Pharmacol.*, **157**, 1045–1052.
31. Pepe, G., Lucarini, L., Zhang, R.Z., Pan, T.C., Giusti, B., Quijano-Roy, S., Gartioux, C., Bushby, K.M., Guicheney, P. and Chu, M.L. (2006) COL6A1 genomic deletions in Bethlem myopathy and Ullrich muscular dystrophy. *Ann. Neurol.*, **59**, 190–195.
32. Lampe, A.K., Zou, Y., Sudano, D., O'Brien, K.K., Hicks, D., Laval, S.H., Charlton, R., Jimenez-Mallebrera, C., Zhang, R.Z., Finkel, R.S. *et al.* (2008) Exon skipping mutations in collagen VI are common and are predictive for severity and inheritance. *Hum. Mutat.*, **29**, 809–822.
33. Lucioli, S., Giusti, B., Mercuri, E., Vanegas, O.C., Lucarini, L., Pietroni, V., Urtizberea, A., Ben Yaou, R., de Visser, M., van der Kooi, A.J. *et al.* (2005) Detection of common and private mutations in the COL6A1 gene of patients with Bethlem myopathy. *Neurology*, **64**, 1931–1937.
34. Steffen, L.S., Guyon, J.R., Vogel, E.D., Beltre, R., Pusack, T.J., Zhou, Y., Zon, L.I. and Kunkel, L.M. (2007) Zebrafish orthologs of human muscular dystrophy genes. *BMC Genomics*, **8**, 79.
35. Dowling, J.J., Vreede, A.P., Low, S.E., Gibbs, E.M., Kuwada, J.Y., Bonnemann, C.G. and Feldman, E.L. (2009) Loss of myotubularin function results in T-tubule disorganization in zebrafish and human myotubular myopathy. *PLoS Genet.*, **5**, e1000372.
36. Bassett, D.I. and Currie, P.D. (2003) The zebrafish as a model for muscular dystrophy and congenital myopathy. *Hum. Mol. Genet.*, **12**(Spec no. 2), R265–R270.
37. Guyon, J.R., Goswami, J., Jun, S.J., Thorne, M., Howell, M., Pusack, T., Kawahara, G., Steffen, L.S., Galdzicki, M. and Kunkel, L.M. (2009) Genetic isolation and characterization of a splicing mutant of zebrafish dystrophin. *Hum. Mol. Genet.*, **18**, 202–211.
38. Hall, T.E., Bryson-Richardson, R.J., Berger, S., Jacoby, A.S., Cole, N.J., Hollway, G.E., Berger, J. and Currie, P.D. (2007) The zebrafish candyfloss mutant implicates extracellular matrix adhesion failure in laminin alpha2-deficient congenital muscular dystrophy. *Proc. Natl Acad. Sci. USA*, **104**, 7092–7097.

39. Thornhill, P., Bassett, D., Lochmuller, H., Bushby, K. and Straub, V. (2008) Developmental defects in a zebrafish model for muscular dystrophies associated with the loss of fukutin-related protein (FKRP). *Brain*, **131**, 1551–1561.
40. Robu, M.E., Larson, J.D., Nasevicius, A., Beiraghi, S., Brenner, C., Farber, S.A. and Ekker, S.C. (2007) p53 activation by knockdown technologies. *PLoS Genet.*, **3**, e78.
41. Lamande, S.R., Shields, K.A., Kornberg, A.J., Shield, L.K. and Bateman, J.F. (1999) Bethlem myopathy and engineered collagen VI triple helical deletions prevent intracellular multimer assembly and protein secretion. *J. Biol. Chem.*, **274**, 21817–21822.
42. Dowling, J.J., Gibbs, E., Russell, M., Goldman, D., Minarcik, J., Golden, J.A. and Feldman, E.L. (2008) Kindlin-2 is an essential component of intercalated discs and is required for vertebrate cardiac structure and function. *Circ. Res.*, **102**, 423–431.